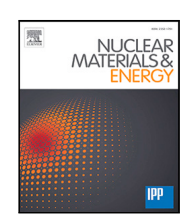
Contents lists available at ScienceDirect

Nuclear Materials and Energy

journal homepage: www.elsevier.com/locate/nme





LIBS depth profiling of Be-containing samples with different gaseous impurity concentrations

P.G. Bhat ^a, P. Veis ^{a,*}, A. Marín Roldán ^a, J. Karhunen ^b, P. Paris ^c, I. Jõgi ^c, A. Hakola ^b, J. Likonen ^b, S. Almaviva ^d, W. Gromelski ^e, M. Ladygina ^e, P. Gasior ^e, J. Ristkok ^c, I. Bogdanović Radović ^f, Z. Siketić ^f, O. Romanenko ^g, C. Porosnicu ^h, C. Lungu ^h

- ^a Department of Experimental Physics, FMPI, Comenius University, Mlynská dolina F2, 842 48 Bratislava, Slovakia
- b VTT, P.O. Box 1000, 02044 VTT, Finland
- ^c Institute of Physics, University of Tartu, W. Ostwaldi str. 1, 50411 Tartu, Estonia
- d ENEA, Frascati research center, via Enrico Fermi, 45, I-00044 Frascati, Italy
- e IPPLM Institute of Plasma Physics and Laser Microfusion, Hery Street 23, 01-497, Warsaw, Poland
- f Rudjer Boskovic Institute, PO Box 180, 10002 Zagreb, Croatia
- 8 Nuclear Physics Institute of the Czech Academy of Sciences, 250 68 Řež, Czech Republic
- h INFLPR 409, Magurele, Jud Ilfov 077125, Bucharest, Romania

ARTICLE INFO

Keywords: LIBS depth profiles Be-containing samples Deuterium Seeding gases Neon detectability Ablation rates

ABSTRACT

Understanding the interaction between the fusion plasma and the plasma-facing materials (PFMs) is crucial for achieving the optimal performance, safety, and lifetime of the fusion devices. Relevant materials have been intensely studied to determine fuel retention and the composition of the co-deposited layers on the PFMs by depth profile analysis using Laser-Induced Breakdown Spectroscopy (LiBs) and Calibration-Free (CF)-LiBs. However, the comparison between the layers containing a mixture of different (seeding) gases using LiBs, has not been studied systematically. Consequently, the aim of this work is the LiBs depth profile analysis of Be-based samples containing the fuel (D) and one of the seeding gases (N, Ne, He) with variable concentrations to study the potential impact on fuel retention in the PFMs. The LiBs measurements were performed using Nd:YAG laser (1064 nm) under Ar atmosphere (at 2 and 100 mbar). In LiBs the ablation rate was evaluated, spectral lines of all relevant elements except N and Ne were detected and compared with the SIMS depth profiles. The reasons for the non-detectability of Ne are discussed in detail.

1. Introduction

In future fusion reactors, one must pay attention to their operational safety. To this end and to ensure smoother yet optimal running of fusion programs, studying the interactions between the Plasma and Plasma Facing Materials (PFMs) is indispensable [1]. For the PFMs in ITER, Be was chosen as the first wall material, while W is foreseen to be used in the divertor.

Laser-Induced Breakdown Spectroscopy (LIBS) has been extensively used to study fusion-relevant materials [2–4]. The Calibration-Free LIBS (CF-LIBS) approach allows for in-depth profiling and quantitative elemental analysis [5], with the ultimate goal of quantifying fuel retention in the inner walls of the reactor [4]. For the development of the methodology of the future online LIBS analyses, especially for analyzing co-deposited layers formed on JET ILW and potentially on ITER, it is important to study different Be-based mixed layers. The first

works on this front were conducted at VTT where the elemental depth profiles were also compared with those obtained using Secondary Ion Mass Spectrometry (SIMS) [6]. Subsequent successful studies dealt, for the first time, with CF-LIBS depth profile analysis by including H/D content quantification in BeWD and AlWD mixed coatings (D concentrations were around 5–6 at.%) [7] and in BeOCD, BeOD, and BeD coatings (D content higher than 20 at.%) [8]. In both cases, the CF-LIBS quantification was compared with other analytical methods like Time-of-Flight Elastic Recoil Detection Analysis (TOF-ERDA) and Ion Beam Analysis (IBA). However, the actual D concentrations based on existing data are generally lower on co-deposited layers (excluding JET – but there, Carbon may be the decisive factor) [9,10]. LIBS investigation of Be coatings at higher pressure are still missing (higher pressure is required for LIBS in ITER during maintenance breaks). Since the scope of this study involves Be-containing samples, which are expected to

E-mail address: pavel.veis@fmph.uniba.sk (P. Veis).

^{*} Corresponding author.

form layers on the reactor walls, the current work focuses mainly on Deuterium (D) profiles. It investigates the impact of the seeding gases concentration (N, He, and Ne) on D LIBS detectability and ablation rates for varying gas pressure. The novelty of this study lies in demonstrating the detection of realistic amounts of D (also verified using TOF-ERDA) through the application of LIBS. These results bring us closer to the actual PFMs found in reactors.

2. Materials and methods

2.1. Samples

The samples consisted of mixed coatings of Be, containing different gases (D, Ne, N, He) at nominal concentrations ranging from 2.5 to 10 at.%, and nominal thicknesses ranging from 5 to 20 μ m (Table 1). These coatings were deposited onto W substrates at the National Institute for Laser, Plasma, and Radiation Physics in Romania using high-power impulse magnetron sputtering (HiPIMS) in a high vacuum chamber [10].

2.2. Experimental setup

The experiments were conducted using a Be-handling LIBS setup at the VTT Technical Research Centre of Finland. A more detailed setup description can be found elsewhere [11], but the key features will be described here. The samples were placed in a vacuum chamber filled with Ar gas to a pressure of 2 or 100 mbar depending on the experiments. A pulsed Nd:YAG laser (Brilliant B, Quantel, 1064 nm, 5 ns) with a fluence of approximately 4.5 J/cm² was used to achieve a low fluence, which is ideal for depth profiling. The emitted light from the plasma plume formed near the sample surface due to the laser pulse was collected perpendicularly to the laser beam using an off-axis parabolic mirror and guided to a fiber bundle consisting of 50 fibers with 50 µm diameters. The fiber bundle was connected to the entrance slit of an Andor SR-750 spectrometer equipped with an Andor iStar 340 T ICCD camera. The spectrometer used in LIBS setup utilized two different gratings [12]: (G1) 600 l/mm grating blazed at 500 nm, giving a wavelength resolution of 0.03 nm and apparatus function width of 0.15 nm with a 40 nm window, used for pre-selected spectral ranges centered at 392 nm, 435 nm, 465 nm, and an additional spectral range depending on the seeding gas, i.e., 587 nm for He, 641 nm for Ne, and 760 nm for N and (G2) 1350 l/mm grating blazed at 675 nm, giving a wavelength resolution of 0.01 nm and apparatus function width of 0.065 nm with a 20 nm window specifically for the H/D spectral window centered at 656 nm. The apparatus function was determined by the He-Ne laser. The delay time and gate width were set to 200 ns for all windows, except for the 656 nm spectral window, where the delay and gate width of 4 µs were used for all the studied samples for a more clear distinction between isotopes. The ICCD camera gain was optimized (varying from 250 to 1500) for different spectral windows to obtain the maximum possible signal without saturating the detector. Spectral lines from higher diffraction orders were avoided by using corresponding bandpass filters. The laser plasma emission was recorded at different distances (Optic's position, OP) from the substrate (3 mm to 6 mm) appropriate to the experimental conditions. The spectra were corrected with the spectral sensitivity (spectral response) and gain of the whole optical system, including the ICCD camera, were corrected. The spectral response was evaluated using a continuous source i.e., the Deuterium lamp for the UV range (200-400 nm) and the Tungsten lamp for the range of 360 nm to 900 nm for all spectral windows. The spectral response is distinct for different gains. While recording the spectral response, the gain of the spectrometer was also varied, thus providing an appropriate set of calibration curves for the studied windows. The recorded spectra from experiments were corrected by dividing the spectral response function corresponding to the gain used while experimenting for a chosen window. The electron temperature

was evaluated using the standard Boltzmann Plot method (temperature (T_e) obtained from the slope of equation Eq. (1)) [5],

$$ln(I_{ki} \times \lambda/A_{ki} \times g_k) = -E_k/k_R \times T_\rho + F \times C_s/U_s(T)$$
(1)

*where I_{ki} , λ , A_{ki} , g_k , E_k , k_B , F, C_s , and $U_s(T)$ are intensity (k^{th} to i^{th} transition), wavelength, transition probability, the degeneracy of the k upper level, Energy of k^{th} level, boltzmann constant, instrumental function, concentration of 's' species, and the partition function, respectively.

The depth profiles for each measurement spot were reconstructed from the kinetic series of 100 laser shots. The elemental intensity profile obtained per shot was mainly fitted to a Lorentzian distribution function while keeping the RMS fitting errors below 20%, typically ranging from 2% to 5%. The intensity profile of H and D lines was deconvoluted, and the area covering the D spectral fitted profile was considered. The obtained integrated area under the fitted intensity profile was recorded for each shot up to 100 laser shots. Hereafter, the "depth profile" refers to the evolution of the intensity of a particular elemental emission line for subsequent 100 laser pulses. We assumed that changes in reflectivity during subsequent pulses are small and have a minor influence on the amount of absorbed energy.

The LIBS results were cross-validated using two other methods: SIMS and TOF-ERDA. The depth measurements for the coatings were recorded by SIMS; the measurement time was converted to depth by determining the thickness of the coatings using a stylus profilometer, which was used for the crater depth evaluation. The signal from the W substrate appeared at depths from 10.43 μm and 9.98 μm for the BeD5 and BeD10Ne5 samples, respectively. The SIMS depth profiles were compared with LIBS depth profiles for ablation rate analysis (Section 3.2). TOF-ERDA [13] was employed to determine the actual concentration (Table 1), which differed from the nominal values. The nominal percentages are used throughout this manuscript, and the terms "at.%" and the "%" symbols are omitted in the sample name.

3. Results and discussions

3.1. Effect of gas pressures on LIBS D/H profiles

The effect of low (2 mbar) and high pressure (100 mbar) conditions on D/H LIBS profiles were studied for a BeD5 sample. The spectra in these experiments were collected at 3 mm from the substrate. The high-pressure conditions led to broadened peak shapes for the D/H doublet, significantly impacting the D peak in the first 10 shots, as observed in the depth profiles. Surprisingly, the D peak was still detectable, albeit weakly, around the 40^{th} shot and onwards (Fig. 1a and the depth profile in the inset). The broadening effect was predominant in the initial ten shots, although the D retention was similar at both pressures, making it challenging to determine the integrated area of the D profile.

3.2. Effect of pressure and gases on the ablation rate

The SIMS depth profiles were already calibrated using independent crater depth measurements (Section 2.2). The ablation rate was calculated by dividing the SIMS thickness of the coatings by the number of LIBS laser shots required to fully penetrate the coating and reach the W substrate (50% of the signal saturation for W substrate in SIMS and LIBS) [14]. The LIBS depth profiles were normalized (divided by maximum) to evaluate the coating and substrate interface. The effect of gas pressures on the ablation rate was studied for the BeD5 coating (LIBS depth profiles in Fig. 1b and SIMS thickness 10.43 μm , Fig. 1c for 100 mbar and Fig. 2a for 2 mbar). The ablation rate was found to be 1.49 μm /shot for 100 mbar pressure and 0.95 μm /shot for 2 mbar pressure, therefore increasing with gas pressure. This result differs from previous studies conducted [15,16], which suggested increased laser energy absorption in a denser plasma plume and the re-deposition of the ablated materials from the previous experiments. Furthermore,

Table 1

Concentration of each species in the samples using TOF-ERDA and thickness of the species determined by SIMS

Sample/coatings	TOF-ERDA (at.%)									Thickness (µm)
	Ве	D	Н	Ne	С	N	0	Ar	He	
BeD5	93	4.5	0.5	_	0.23	0.26	0.9	_	_	8.22
BeD10Ne2.5	94	3.9	0.36	_	0.13	0.53	0.9	-	_	10.8
BeD10Ne5	88	8.5	0.33	0.29	0.13	0.95	0.56	0.3	-	9.17
BeD5He2.5	95	1.1	0.6	_	0.25	0.6	0.12	-	0.54	N/A
BeD5He5	89	3.7	1.1	-	0.29	0.9	1.3	0.14	2.8	N/A

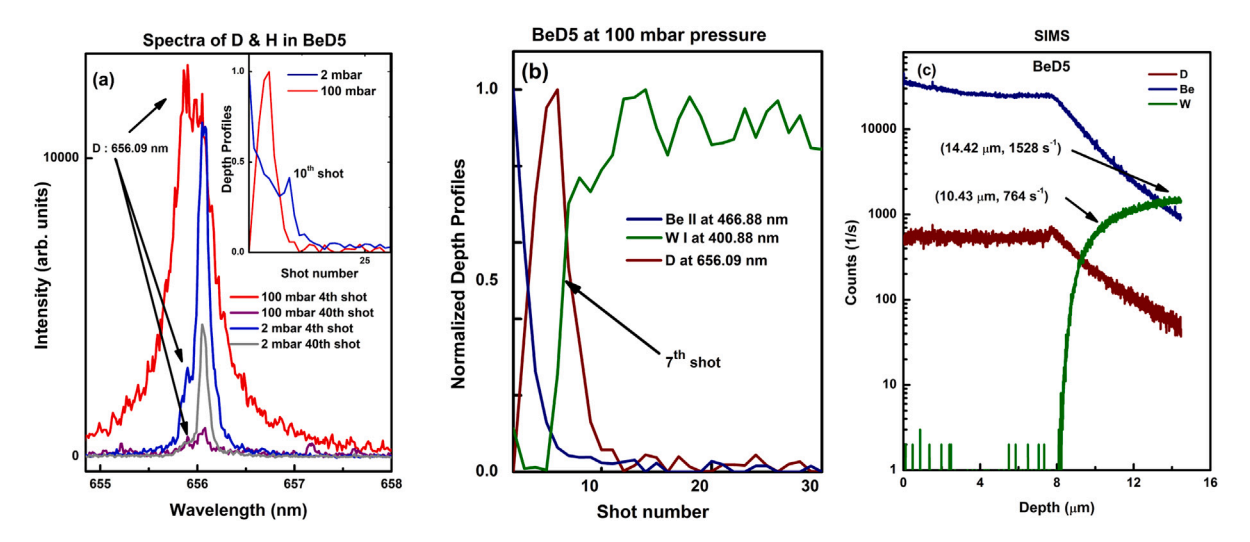


Fig. 1. BeD5 sample's (a) Spectra at 2 mbar and 100 mbar with inset showing the LIBS depth profiles (b) LIBS depth profiles of Be II (466.88 nm), W I (400.88 nm), and D (656.09 nm) at 100 mbar pressure (c) SIMS depth profiles showing the thickness of the coating around 10.43 μm.

the influence of Ne (5%) gas inclusion (Fig. 2b : OP at 6 mm from the sample, and SIMS thickness 9.98 μ m Fig. 2c) on the ablation rate under low-pressure conditions was investigated and was found to be 0.42 μ m/shot. The prepared samples originated from different batches and thus differed in D content (TOF-ERDA: D = 8.5%) in comparison to the sample without Ne seeding. The previous studies conducted on W coatings show the ablation rate to be mainly dependent on the composition, density (eventually porosity), and deuterium content in the samples [6,14]. Previous studies with an increase in D content led to an increased ablation rate [6,14]. In our case, we found approximately 45% decrease in the ablation rate with Ne inclusion at 2 mbar pressure, indicated by the elemental interface reached at the 24th shot (Fig. 2c). This decrease in the ablation rate signifies the role of the composition of the samples on the ablation rate.

3.3. Effect of different gases on D depth profiles

The effect of different seeding gases and He on the D depth profiles was investigated for coatings with varying elemental nominal concentrations (Fig. 3a). Although the spectra from samples containing N (BeD5N2.5, TOF-ERDA: Be = 96%, D = 2.1%, N = 0.68%) were recorded, D was not detectable in LIBS spectra. At the same time, D was clearly detectable in BeD5He2.5 coating, which contained 1.1% deuterium. This suggests that the D detectability depends on the investigated material. The samples with Ne for D profiles in this section are not considered as they were measured only at a higher pressure of 100 mbar (Fig. 2b). As a result, the following coatings were considered: BeD5 (OP at 3 mm), BeD5He2.5 (OP at 6 mm), and BeD5He5 (OP at 6 mm). An interesting finding was a spike in D intensity which was observed around the 10^{th} shot for BeD5 (TOF-ERDA: Be = 93%, D = 4.5%) and the 9th shot for BeD5He2.5 (TOF-ERDA: Be = 95%, D = 1.1%), corresponding to the interface between Be coating and W substrate. This spike may indicate the influence of various parameters, such as differences in ablation rate, plasma plume electron density

and plasma temperature between the coating and substrate, variations in the matrix, and possible accumulation of D at the interface of the coatings and substrate [8]. Interestingly, this spike was not observed in the sample containing nominally 5% He (Fig. 3a, TOF-ERDA: Be = 89%, D = 3.7%) and 2.5% Ne (TOF-ERDA: Be = 94%, D = 3.9%, Fig. 2b). The electron density determined from the FWHM value of D and H lines increased for the laser shots 8–9 in the case of BeD5He2.5 coating, where the D spike was most pronounced, while such an increase was not detectable for other coatings. This suggests that the change in plasma parameters may partially explain the spike for this particular coating, but further systematic experimentation is needed to address this specific question.

3.4. LIBS detectability of Ne, N, and He in Be-based samples under Ar low-pressure atmosphere

Systematic studies on detecting Neon, Nitrogen, and Helium spectral lines in optical emission spectra (OES) of laser-induced plasma where these impurities originate from the Be samples are not reported in the literature. Spectra simulations using available spectral line data indicate that the most intense Ne line is located at 640.21 nm, He line at 587.56 nm, and N lines at 742.36, 744.23, and 746.83 nm [17]. We analyzed LIBS spectra of the BeD10Ne5, BeD5He2.5, and BeD5N2.5 samples (refer Section 2.2, TOF-ERDA Table 1). We were unable to detect Ne, He, nor N using the mentioned LIBS conditions while the Ne content was 0.29%, He content 0.54% and N content 0.68% in the coatings according to TOF-ERDA (Table 1), nominal contents are listed in sample name. At the same time, the He 587.56 nm line was clearly detectable in the BeD5He5 sample, which contained 2.8% He according to TOF-ERDA. This suggests that the detection of the seeding gases Ne and N and fusion reaction product He with a concentration below 1% in Be-containing samples requires additional effort and analysis of the plasma plume properties. Fig. 4 presents the most prominent Be I-II, W I-II, and Ar II spectral lines in the LIBS spectrum recorded for the

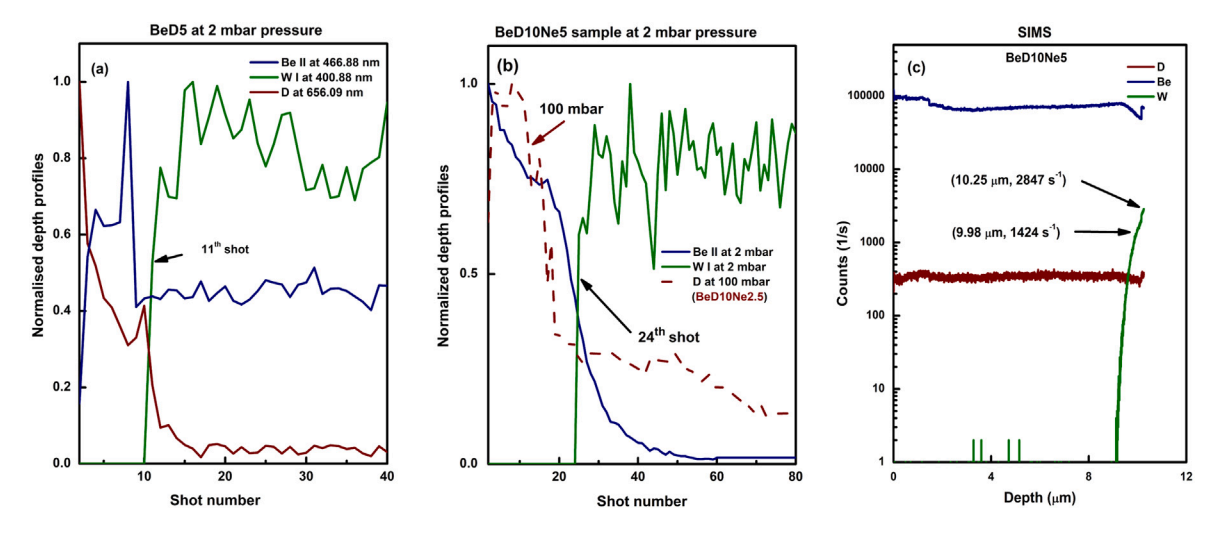


Fig. 2. LIBS depth profiles Be II (466.88 nm), W I (400.88 nm), and D (656.09 nm) at 2 mbar pressure for (a) BeD5 (b) BeD10Ne5, dashed: D profile (100 mbar, BeD10Ne2.5 sample) and (c) BeD10Ne5 SIMS depth profiles with the thickness of the coating around 9.98 µm.

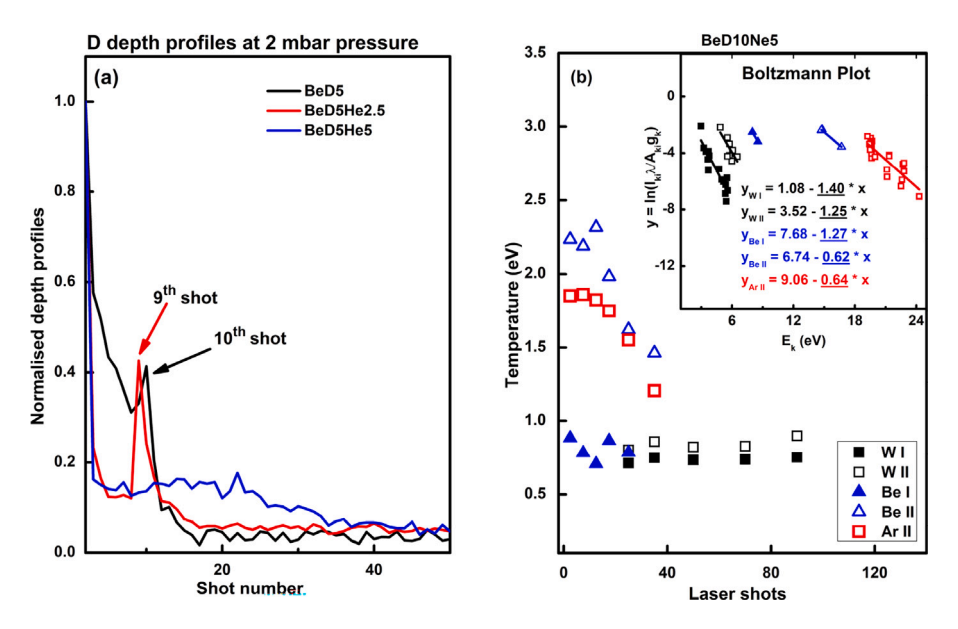


Fig. 3. (a) D depth profiles at 2 mbar pressure for samples BeD5, BeD5He2.5, and BeD5He5 and (b) the evolution of T_e with respect to laser shots obtained for BeD10Ne5 at 2 mbar pressure and inset showing the Boltzmann Plot.

BeD10Ne5 sample under an Ar pressure of 2 mbar. The spectra were averaged for different numbers of laser shots with depth. In the first four averaged spectra within the layer, only Be I-II, and Ar II spectral lines are present. In the subsequent spectra, W I-II lines appear while Be I-II and Ar II lines gradually disappear. We examined the depth evolution of electron temperature (T_e) Fig. 3b using Boltzmann plots calculated from averaged spectra (Fig. 4). The $T_{\it e}$ obtained from the averaged spectra in the BeD10Ne5 coating from Ar II lines is T_e = 1.8 eV, while in the W substrate, it was 0.77 eV according to W I-II lines. The T_e , according to Ar II lines, started to decrease at the interface between the BeD10Ne5 layer and W substrate (shots 21-30) but remained still higher than the temperature determined from W I-II lines. Similar results were obtained for other Be-containing coatings (the T_e in N-containing coatings was not analyzed). Spectra simulations using the T_a determined from Ar II lines and assuming LTE conditions [17] are in line with the absence of Ne, and He lines when the concentration remains below 1%. The graph Fig. 3b demonstrates that the Ar II and W I-II lines are populated differently as the obtained T_e of these two elements differs. The difference may be caused by the population of the emitting Ar II levels from higher Ar II levels created

by recombination which exceeds the non-equilibrium conditions [18] and/or in the case of Ne and He containing samples by the collisional energy transfer from excited Ne and He states which have higher energy than Ar II levels.

4. Conclusions

Realizing the importance of Be-based mixed layers with various seeding gases for the future online LIBS analysis of JET with ITER-like wall reactors, the current work investigates the effect of composition, pressure, and ablation rates on D-containing samples. The effect of Ar gas pressure (2 mbar and 100 mbar) was studied on the samples containing Be and D. At the pressure of 100 mbar, the H/D profile was broadened, making it challenging to accurately determine and allocate peaks. The effect of pressure on the ablation rate was also studied. It was observed that the ablation rate increased with pressure. Inclusion of 0.29 at.% Ne (BeD10Ne5) decreased the ablation rate and increased D content from 3.9 at.% to 8.5 at.%, relative to the sample BeD5. The exact parameters influencing this effect are currently unknown as the material's properties, such as porosity and heat transfer, may vary

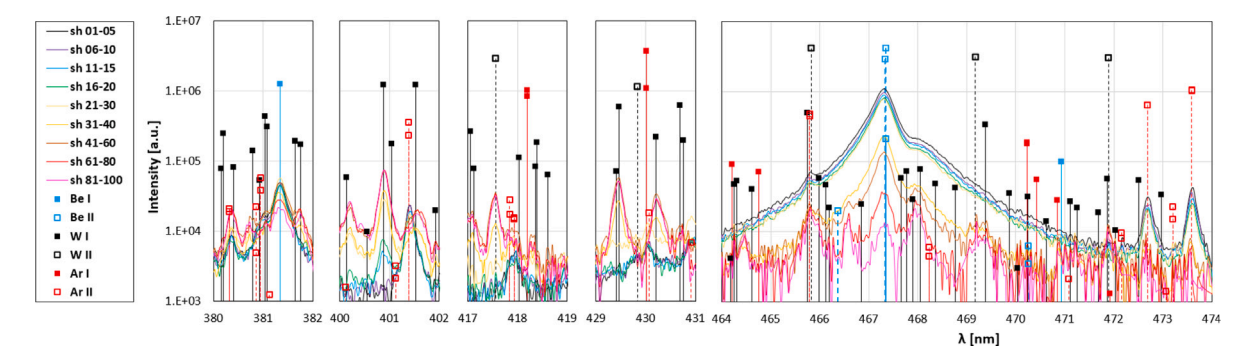


Fig. 4. LIBS spectrum of the BeD10Ne5 sample recorded under an Ar atmosphere at a gas pressure of 2 mbar, with different spectral ranges highlighted: (a) 380–382 nm (Be I at 381.35 nm), (b) spectral range 400–402 nm (W I at 400.87 nm and 401.52 nm, Ar II and 401.38 nm), (c) spectral range 417–419 nm (W II at 417.56 nm), (d) spectral range 429–431 nm (W I at 429.46 nm and 430.21 nm), and (e) spectral range 464–474 nm (Be II at 467.34 nm, Ar II at 472.69 nm and 473.59 nm). The spectra were averaged after different numbers of laser shots, initially in the layer averaging every 5 shots (1–5, 6–10, 11–15, 16–20) and later in the tungsten substrate averaging every 10 shots (21–30, 31–40) and every 20 shots (41–60, 61–80, 81–100).

and require further experimentation. The effect of different gases on D profiles was investigated, and D content of 2.1 at.% in the case of BeD5N2.5 was not detectable, although D content down to 1.1%, was still detectable using LIBS and reported in this study. This suggests that D detectability depends on the investigated material and, more in general, that matrix effects could affect this detectability. A spike in the LIBS depth profiles was observed around 9th and 10th shots for samples with less than 5% nominal He content. This spike may indicate impurities at the boundary between the coatings and the substrate or matrix effects at the interfaces of two different materials. Ne, N, and He were not detectable in the LIBS spectra when the concentration remained below 1%. Spectra simulations assuming the LTE condition and using the electron temperatures determined from Ar II lines also suggest the absence of Ne, and He lines when the concentration remains below 1%. Coatings with higher impurity concentrations are required to further investigate the LIBS ability to detect the seeding gases and He in the Be-containing coatings.

CRediT authorship contribution statement

P.G. Bhat: Writing – original draft, Formal analysis, Methodology, Visualization, Software. P. Veis: Investigation, Visualization, Data analysis and interpretation, Writing - review & editing. A. Marín Roldán: Data curation: LIBS experiments, Investigation, Writing - review & editing. J. Karhunen: Data curation: LIBS experiments, Review. P. Paris: Data curation: LIBS experiments, Investigation, Data analysis, Review & editing. I. Jõgi: Visualization, Validation, Writing - review & editing. A. Hakola: Data curation: LIBS and SIMS experiments, Writing - review & editing. J. Likonen: Data curation: SIMS experiments, Review. S. Almaviva: Data curation: LIBS experiments, Review & editing. W. Gromelski: Data curation: LIBS experiments, Review & editing. M. Ladygina: Review & editing. P. Gasior: Review & editing. J. Ristkok: Data curation: LIBS experiments, Review & editing. I. Bogdanović Radović: Data curation: TOF-ERDA results. Z. Siketić: Data curation: TOF-ERDA experiments. O. Romanenko: Data curation: TOF-ERDA experiments. C. Porosnicu: Sample preparation. C. Lungu: Sample preparation.

Declaration of competing interest

The authors declare that they have no known competing financial interests or personal relationships that could have appeared to influence the work reported in this paper.

Data availability

Data will be made available on request.

Acknowledgments

This work has been carried out within the framework of the EU-ROfusion Consortium, funded by the European Union via the Euratom Research and Training Programme (Grant Agreement No 101052200 - EUROfusion). Views and opinions expressed here are however those of the author(s) only and do not necessarily reflect those of the European Union or European Commission. Neither the European Union nor the European Commission can be held responsible for them. The authors PGB, PV, and AMR acknowledge the Scientific Grant Agency of the Slovak Republic (contract number 1/0803/21, VEGA-2/0144/21) and the Slovak Research and Development Agency (APVV-16-0612 and APVV-22-0548) for financial support. This scientific paper has been published as part of the international project co-financed by the Polish Ministry of Science and Higher Education within the programme called 'PMW' for 2023.

References

- R. Wenninger, R. Albanese, R. Ambrosino, et al., The DEMO wall load challenge, Nucl. Fusion 57 (2017) 1–11.
- [2] C. Li, C.L. Feng, H.Y. Oderji, et al., Review of LIBS application in nuclear fusion technology, Front. Phys. 11 (2016) 114214.
- [3] G.S. Maurya, A. Marín-Roldán, P. Veis, et al., A review of the LIBS analysis for the plasma-facing components diagnostics, J. Nucl. Mater. 541 (2020) 152417.
- [4] H. van der Meiden, S. Almaviva, J. Butikova, et al., Monitoring of tritium and impurities in the first wall of fusion devices using a LIBS based diagnostic, Nucl. Fusion 61 (2021) 125001.
- [5] A. Ciucci, M. Corsi, V. Palleschi, et al., New procedure for quantitative elemental analysis by laser-induced plasma spectroscopy, Appl. Spectrosc. 53 (1999) 960–964.
- [6] J. Karhunen, A. Hakola, J. Likonen, et al., Development of laser-induced breakdown spectroscopy for analyzing deposited layers in ITER, Phys. Scr. 2014 (T159) (2014) 014067.
- [7] P. Veis, A. Marín-Roldán, V. Dwivedi, et al., Quantification of H/D content in Be/W mixtures coatings by CF-LIBS, Phys. Scr. 2020 (T171) (2020) 014073.
- [8] V. Dwivedi, A. Marín-Roldán, J. Karhunen, et al., CF-LIBS quantification and depth profile analysis of be coating mixed layers, Nucl. Mater. Energy 27 (2021) 100000
- [9] K. Heinola, J. Likonen, T. Ahlgren, et al., Long-term fuel retention and release in JET ITER-like wall at ITER-relevant baking temperatures, Nucl. Fusion 57 (2017) 1 11
- [10] A. Hakola, K. Heinola, K. Mizohata, et al., Effect of composition and surface characteristics on fuel retention in beryllium-containing co-deposited layers, Phys. Scr. 2020 (T171) (2020) 014038.
- [11] J. Karhunen, A. Hakola, J. Likonen, et al., Applicability of LIBS for in situ monitoring of deposition and retention on the ITER-like wall of JET - comparison to SIMS, J. Nucl. Mater. 463 (2015) 931–935.
- [12] J. Karhunen, Spectroscopic Measurements of Impurity Migration, Deposition and Fuel Retention in Fusion Devices (Doctoral thesis), Aalto University School of Science, 2018, pp. 154–157, URL: http://urn.fi/URN:ISBN:978-952-60-7984-4.

- [13] Z. Siketić, N. Skukan, I. Bogdanović Radović, A gas ionisation detector in the axial (Bragg) geometry used for the time-of-flight elastic recoil detection analysis, Rev. Sci. Instrum. 86 (8) (2015) 083301.
- [14] M. Suchoňová, P. Veis, J. Karhunen, et al., Determination of deuterium depth profiles in fusion-relevant wall materials by nanosecond LIBS, Nucl. Mater. Energy 12 (2017) 611–616.
- [15] N. Farid, H. Wang, C. Li, et al., Effect of background gases at reduced pressures on the laser treated surface morphology, spectral emission and characteristics parameters of laser produced Mo plasmas, J. Nucl. Mater. 438 (2013) 183–189.
- [16] N. Farid, S.S. Harilal, H. Ding, A. Hassanein, Emission features and expansion dynamics of nanosecond laser ablation plumes at different ambient pressures, J. Appl. Phys. 115 (2014) 033107.
- [17] A. Kramida, Y. Ralchenko, J. Reader, N.A. Team, NIST atomic spectra database (version 5.10), [online], 2022, URL: https://physics.nist.gov/asd.
- [18] G. Cristoforetti, A.D. Giacomo, M. Dell'Aglio, et al., Local thermodynamic equilibrium in laser-induced breakdown spectroscopy: Beyond the McWhirter criterion, Spectrochim. Acta B 65 (2010) 86–95.